Processing of the 2010 field school 3D and 2D seismic data from Priddis, Alberta

J. Helen Isaac and Don C. Lawton

ABSTRACT

We processed the vertical component of 2D3C and 3D3C seismic data acquired at field schools near Priddis, Alberta, in 2010. The processing was designed to attenuate noise and enhance signal, especially in the section of interest above 0.5 s. Data quality is good, especially on the high fold prestack time migrated 2D line, where reflections can be seen almost to the surface in the western end of the line. The gentle easterly dip of the Neogene Paskapoo Formation and Early Cretaceous Edmonton Group can be seen above 0.5 s on the processed data. The Paskapoo Formation and Edmonton Group strata dip to the east above the upper detachment while deeper in the section, below the lower detachment which is just above the top of the Belly River, the reflections are sub-parallel. The top of the Mississippian carbonates is imaged at about 1.7 s.

INTRODUCTION

A 3D3C survey was acquired in May, 2010 and a 2D3C survey was acquired in August, 2010 during student field school on university lands close to the Rothney Astronomical Observatory near Priddis, Alberta (Figure 1). The 3D survey covers a slightly larger area than did the 3D acquired in 2007. The survey consists of 514 usable shots from a mini-vibrator source acquired at 10 m intervals along fifteen north-south shot lines and recorded by 514 three-component geophones planted at 10 m intervals along seven west-east receiver lines. The data were binned into 5 m x 5 m cdp bins having an average fold of 60 along 62 inlines and 132 crosslines (Figure 2). The acquisition parameters were chosen for optimal imaging of the shallow section (above 1 s) thus the farthest source-receiver offsets in the data were less than 800 m.

The 2D3C survey was designed to cross the ridge to the west of the observatory (Figure 1) with the hope of being able to correlate the outcropping sands with reflections on the seismic data. A mini-vibrator source was used to acquire 628 usable shots. The data were recorded on a maximum of 488 channels per shot from a 588-channel 3C geophone spread with average offsets of 1000 m and farthest offsets of 2400 m.

The 2D line went up the road allowance and across a rancher's land up the ridge, which presented difficulties with changes in elevation, navigation through trees and shrubs, and surveying (Figures 2 and 3). There was a small lateral shift of a few metres in the line when it moved from the road allowance onto the rancher's land to ascend the hill. It also crossed a road, leaving a 10 station gap in the receiver coverage. There were some issues with shot station assignment as the shot stations annotated in the observer's notes did not always agree with the shot station as suggested by the first breaks. In cases of discrepancy we based the shot stations on the first breaks. The CDP fold is so great that a few improperly positioned shots would not have a noticeable effect on the stacked data. The fold is over 100 for 86% of the line and reaches 350 in the centre (Figure 4b). Issues with the GPS navigation are discussed in Hall et al. (2010).

DATA PROCESSING

We processed the vertical component of both data sets using a standard processing stream (Tables 1 and 2) in ProMAX, concentrating on the removal of noise, data enhancement and augmentation of high frequencies, especially in the 3D data set. We applied almost the same processing procedures to each data set. The CDP fold map for the 3D data is displayed in Figure 4a. Representative 3D shot gathers and 2D shot gathers before and after processing are displayed in Figures 5 and 6, respectively. Only the first 1 s of the 3D data is shown. Much of the noise has been attenuated and shallow reflections are seen. The raw data contained signal frequencies up to 100 Hz with the predominant frequencies being in the 20-45 Hz range. Both predictive and Gabor deconvolution (Margrave and Lamoureux, 2002) were applied to the data. Reflections are seen in the zone of interest at 0.2-0.3 s and 0.4-0.5 s. The 2D data contain many events other than the P-wave reflections of interest but these have not been investigated at present as our priority is to obtain imaging of the shallow P-wave reflectors.

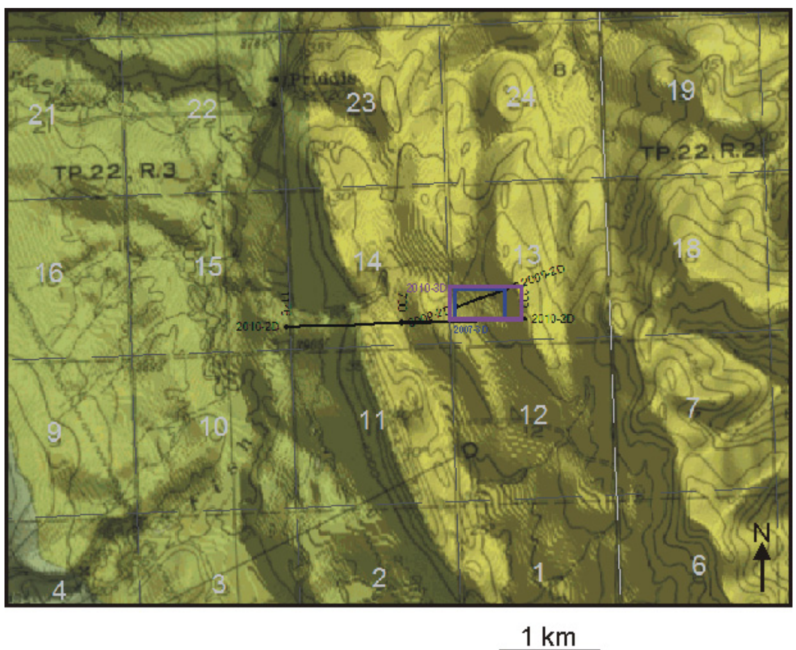

FIG. 1. Location of the 2010 field school 2D and 3D seismic surveys (map after GSC, 1941).

Stacking the 3D data into azimuthal bins shows that data with dip (almost east-west) source-receiver azimuths are less noisy than those of strike (almost north-south) azimuth and are able to image a reflection at 0.95 s. In Figure 7a the azimuths included in the stack are 43°-133° and 223°-313° (dip direction) while in Figure 7b the azimuths included are 313°-43° and 133°-223° (strike direction). Poststack migrated and prestack migrated versions of a 3D inline across the middle of the 3D survey are shown in Figures 8a and 8b, in which the full 2 s of data are shown. AGC was applied to enhance the display of the deeper reflections. The same velocity model, which was derived from stacking velocities, was used for both migrations, which were done from the final datum of 1260 m.

FIG. 2. View down the 2D line.

Table 1. Processing sequence for the 3D data.

3D geometry assignment and binning
Elevation and refraction statics
Geometric spreading compensation; surface consistent amplitude scaling
Surface wave noise attenuation; air blast attenuation
Predictive deconvolution
Q-compensation
Gabor deconvolution
Spectral balance
Bandpass filter 5-10-90-100 Hz
Velocity analysis
Residual statics
Post stack time migration
Pre stack time migration
Pre stack depth migration

FIG. 3. The vibrator truck navigates up the ridge.

Table 2. Processing sequence for the 2D data.

2D geometry assignment and binning
Elevation and refraction statics
Geometric spreading compensation; surface consistent amplitude scaling
Surface wave noise attenuation; air blast attenuation; spike and noise removal
Predictive deconvolution
Q-compensation
Gabor deconvolution
Bandpass filter 5
Velocity analysis
Residual statics
Post stack time migration
Pre stack time migration

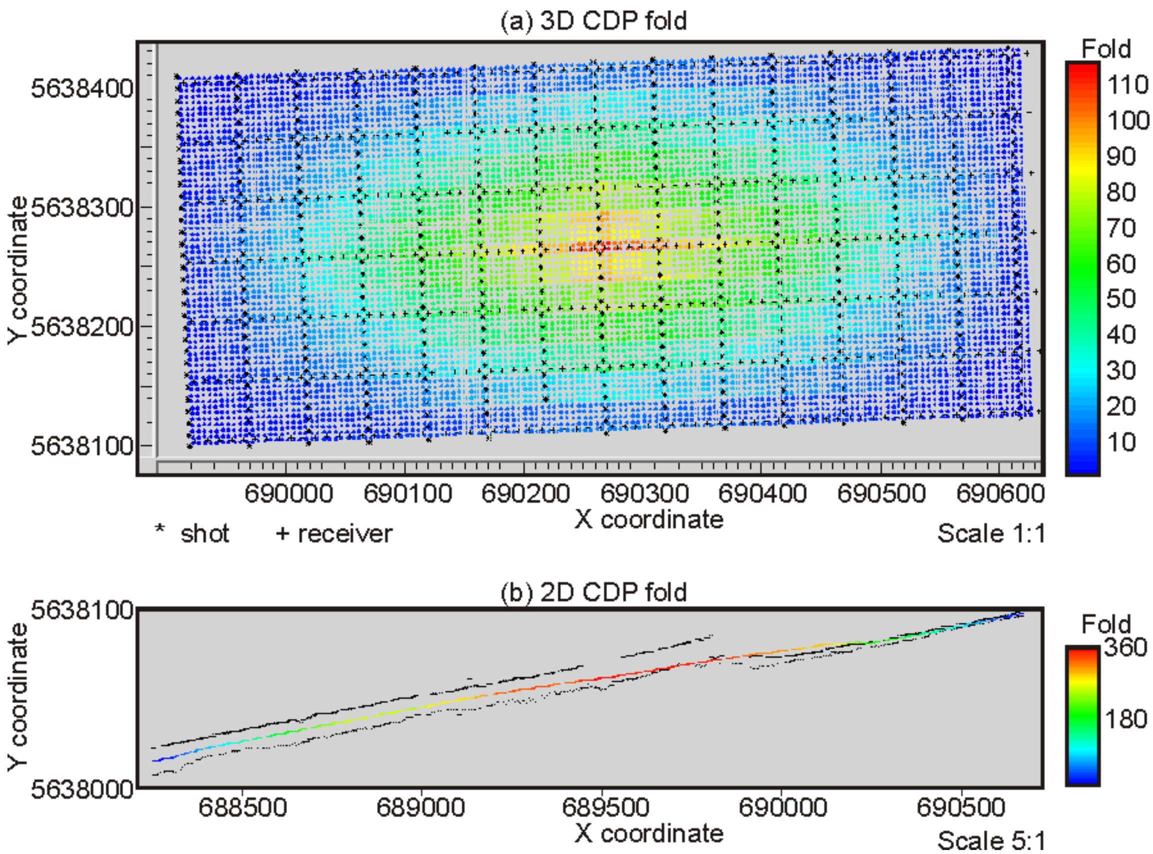

FIG. 4. CDP fold map for the (a) 3D survey and (b) 2D survey.

The gentle easterly dip of the Paskapoo and Edmonton formations can be seen above 0.5 s. The top of the Mississippian carbonates is imaged at about 1.7 s and is a cleaner reflection on the prestack section than on the poststack, and the very shallow section is much more interpretable on the prestack section. Two inlines with zoomed images of the shallow section are presented in Figure 9. An AGC was applied to enhance visibility of the shallowest reflections, which can be seen as shallow as 50 ms in the centre of the liens.

Poststack migrated and prestack migrated versions of the 2D line are shown in Figures 10a and 10b. The prestack migration shows excellent imaging of the shallow reflectors of interest and a clear distinction between the dipping Paskapoo and Edmonton Group strata and the deeper undeformed Belly River and older strata

The event we term the Middle Paskapoo sand is best imaged on the 3D data at 0.22-0.3 s, where the reflections are very strong. The event is also seen on the 2D data but cannot be followed reliably above about 0.15 s. The Lower Paskapoo sand is well imaged on the 2D line, where it can be seen to dip from 0.1 s in the west to 0.45 s near the eastern end of the line. Bandlimited and zoomed versions of the 2D lines give the best images of the very shallow dipping reflectors (Figure 11). These data were filtered with a bandpass filter of 25-30-80-90 Hz and an AGC of 300 ms was applied. The prestack data has been muted above 0.05 s to remove the high amplitude migration artefacts observed on the prestack migrated gathers.

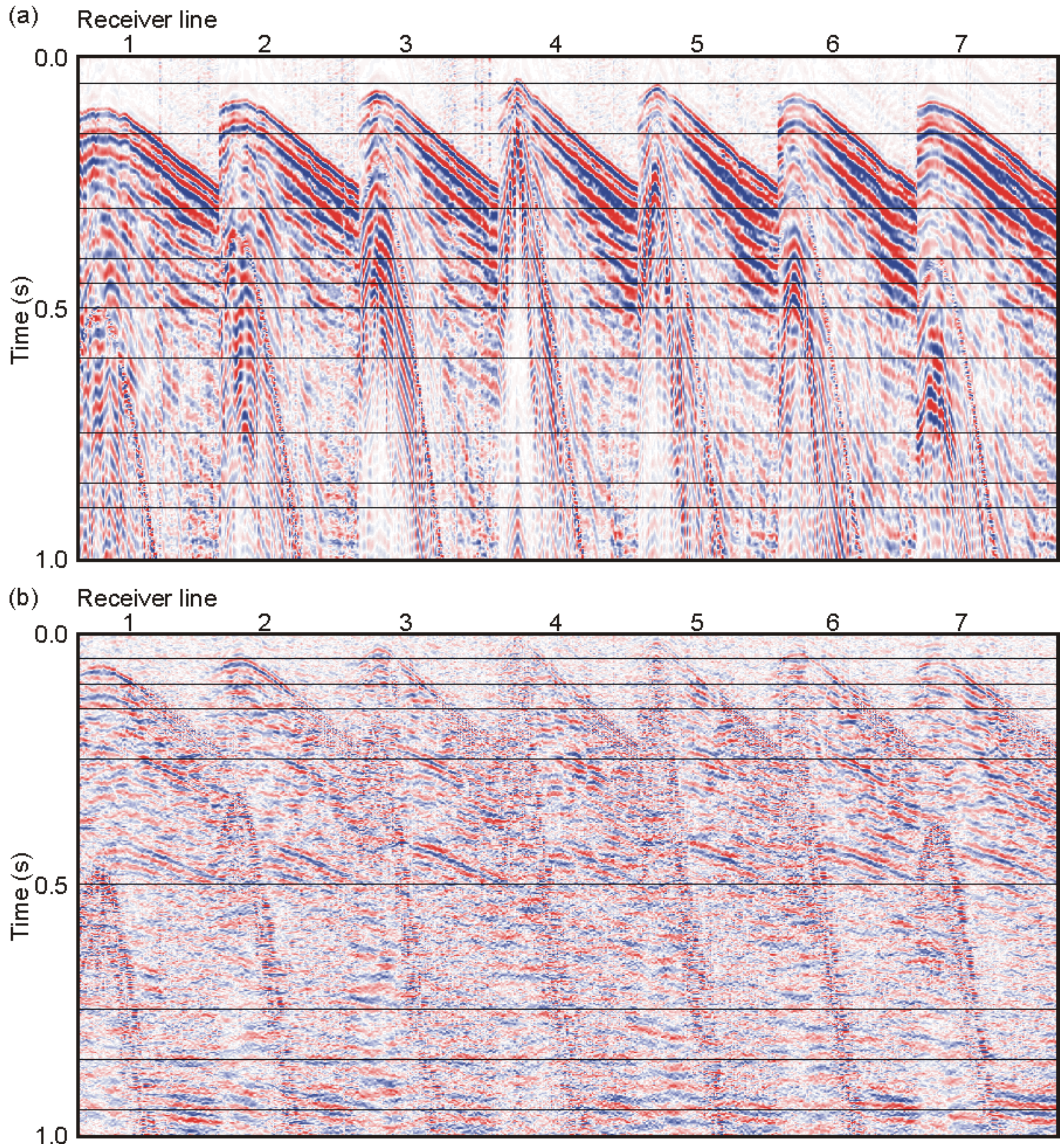

FIG. 5. Representative shot gathers for the seven receiver lines. (a) The field data with an AGC applied and (b) the same gathers after all pre-stack processing. Surface wave noise has been attenuated and we are able to see reflections in the zone of interest above 0.5 s.

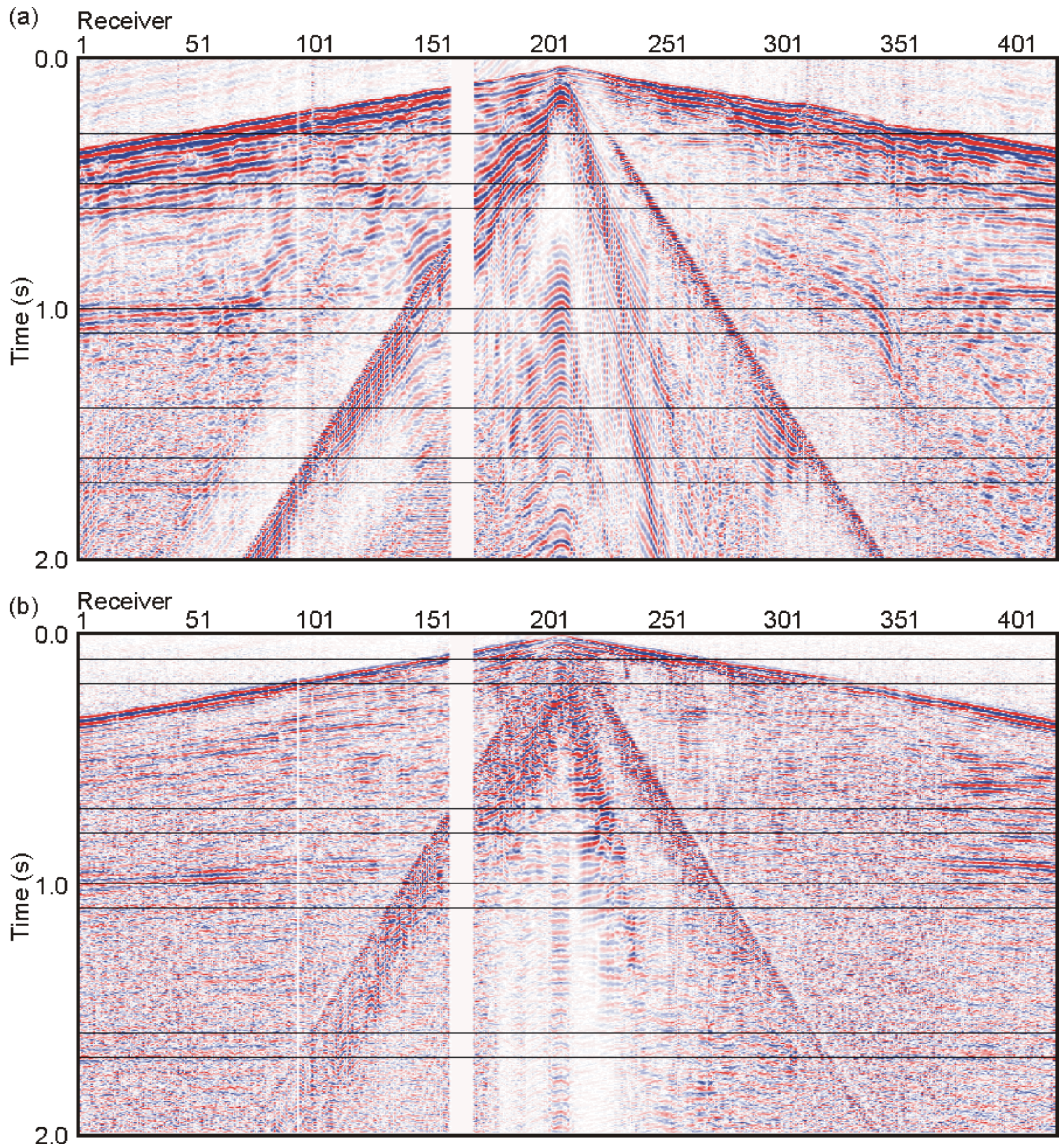

FIG. 6. A representative shot gather from the vertical component of the 2D survey. (a) The field data with an AGC applied and (b) the same gather after all pre-stack processing. The various forms of surface wave noise and other unwanted waves have been attenuated and we are able to see reflections in the zone of interest above 0.5 s. The receiver gap occurs where the line crossed the road.

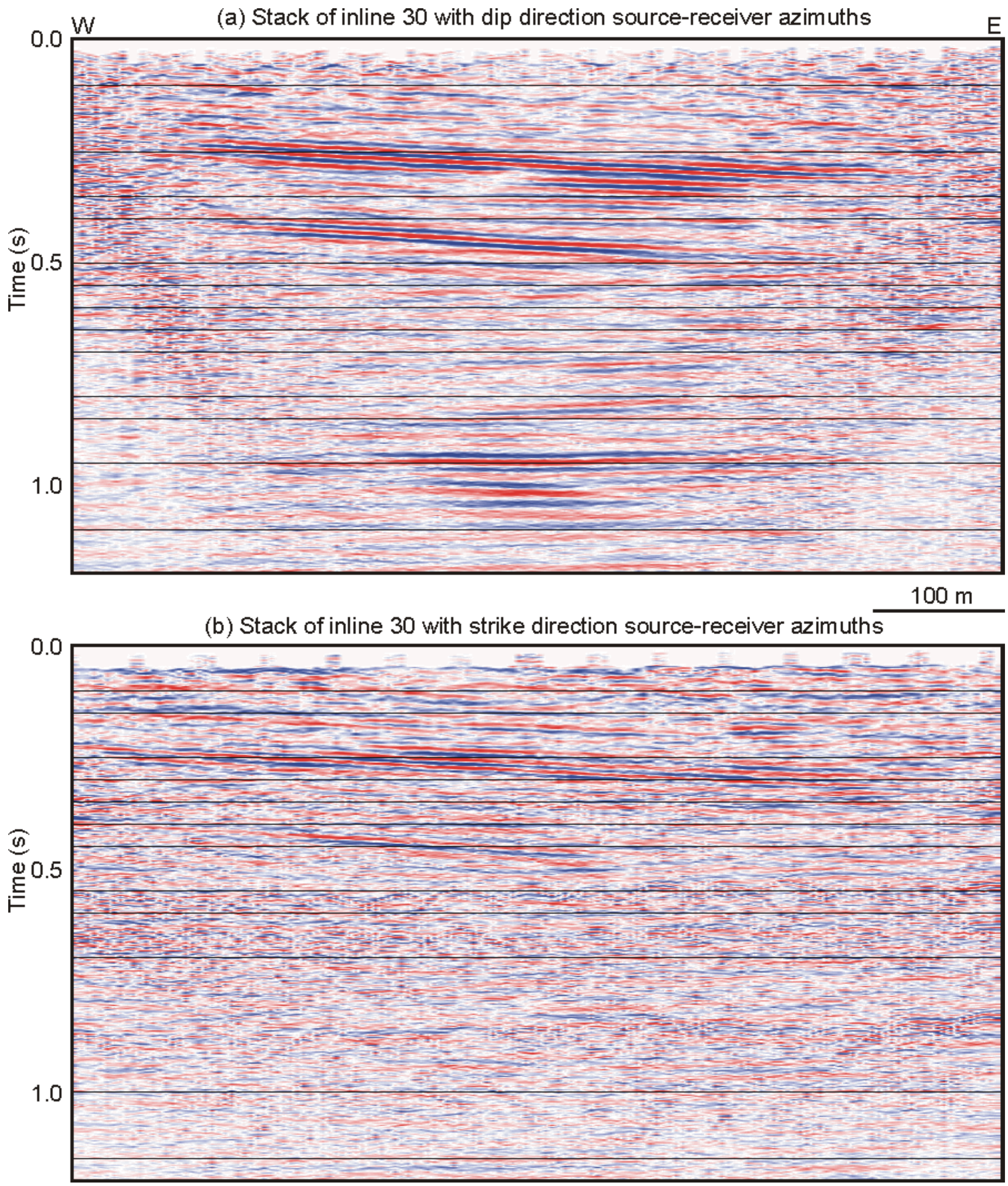

Fig. 7. Inline 30 from the 3D survey stacked using specific offsets. The stacked with offsets from the dip direction (a) shows much more signal than does the stack with offsets from the strike direction.

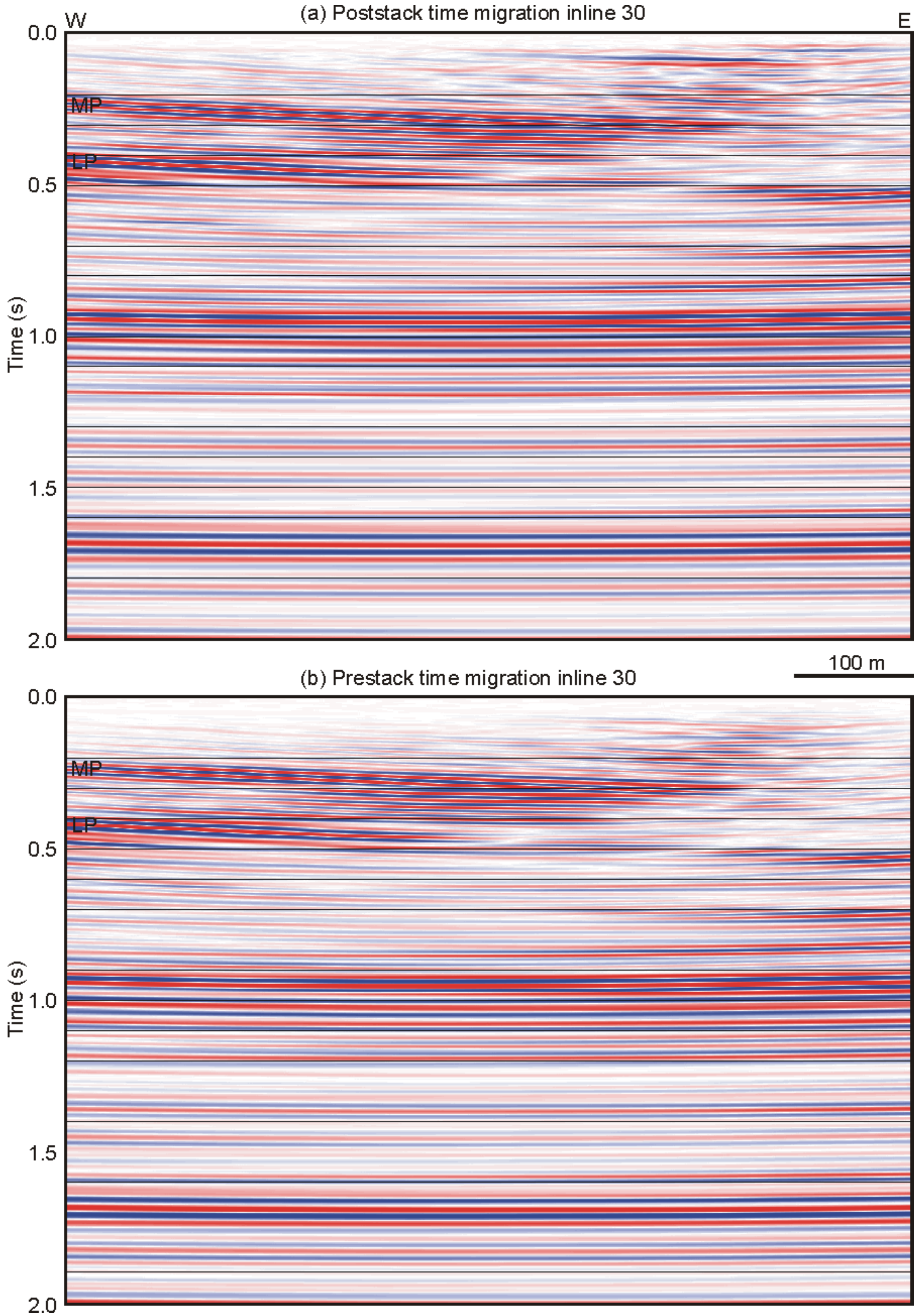

Fig.8. (a) Poststack and (b) prestack time migrated inline 30 from the 3D survey. . MP and LP denote the Middle Paskapoo and Lower Paskapoo sands, respectively.

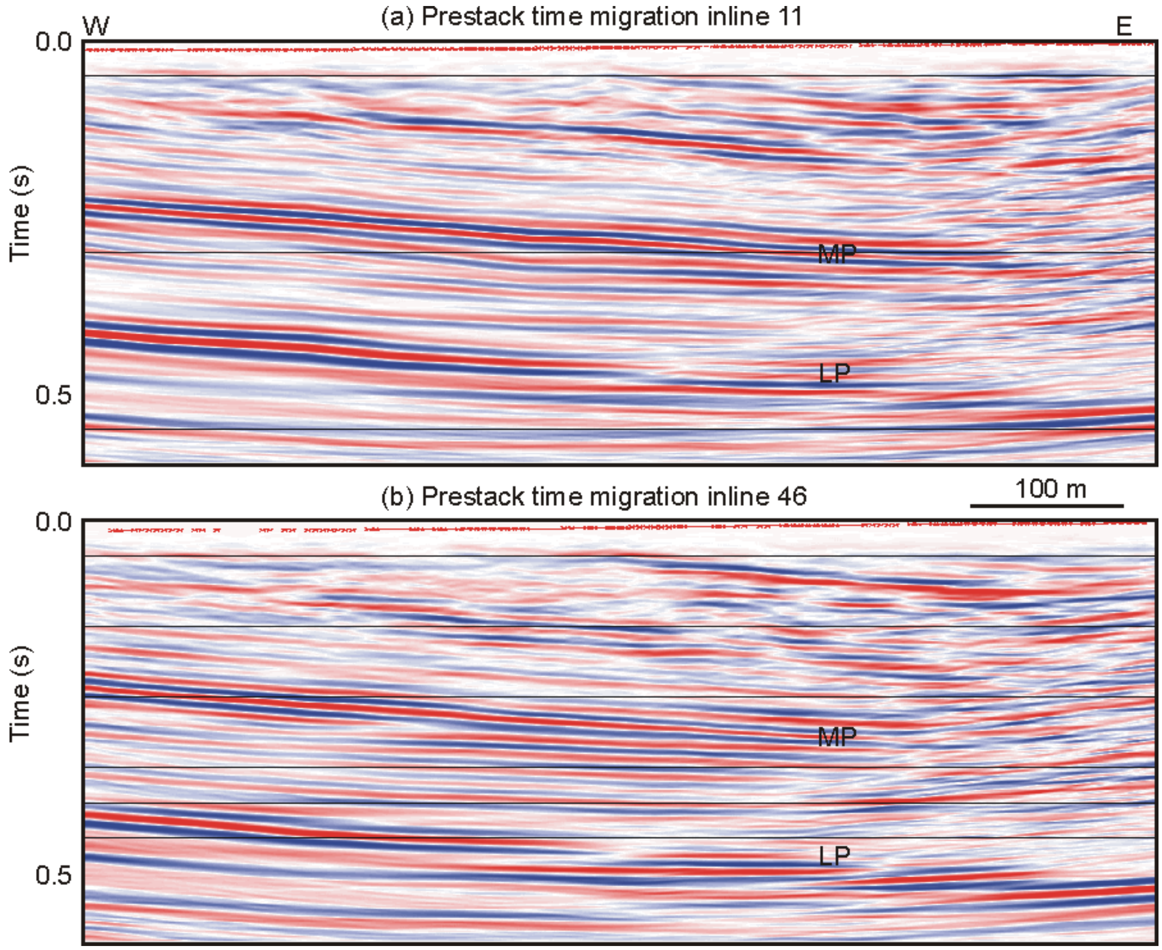

FIG. 9. Zoomed versions of two prestack time migrated inlines from the 3D survey with an AGC of 300 ms applied. The surface is represented by the red crosses. Reflections can be seen as shallow as 50 ms in the centre of the lines. MP and LP denote the Middle Paskapoo and Lower Paskapoo sands, respectively.

We also prestack depth migrated the 3D data using a simple layered interval velocity model in GeoDepth. Figure 12 shows inline 30. The offsets were not long enough to allow us to perform an adequate residual velocity moveout analysis for the reflections on depth gathers. However, the interval velocity from surface to the Middle Paskapoo reflection of 3500 m/s obtained from wells logs worked well as an imaging velocity.

Interpretation of the data and its integration into the existing geological model is discussed in the accompanying paper (Isaac and Lawton, 2010).

We have taken a preliminary look at the converted-wave 2D data, which show various compressional- and shear-wave events. Figure 13 displays a PS shot gather before and after some filtering of low velocity events. Elevations statics and shot refraction statics have been applied to the gather in Figure 13b. We will pursue improvement of the data through application of receiver refraction statics, further signal enhancement techniques and PS velocity analysis. The 3D3C data are heavily contaminated with noise and we were unable to detect PS converted-wave signal.

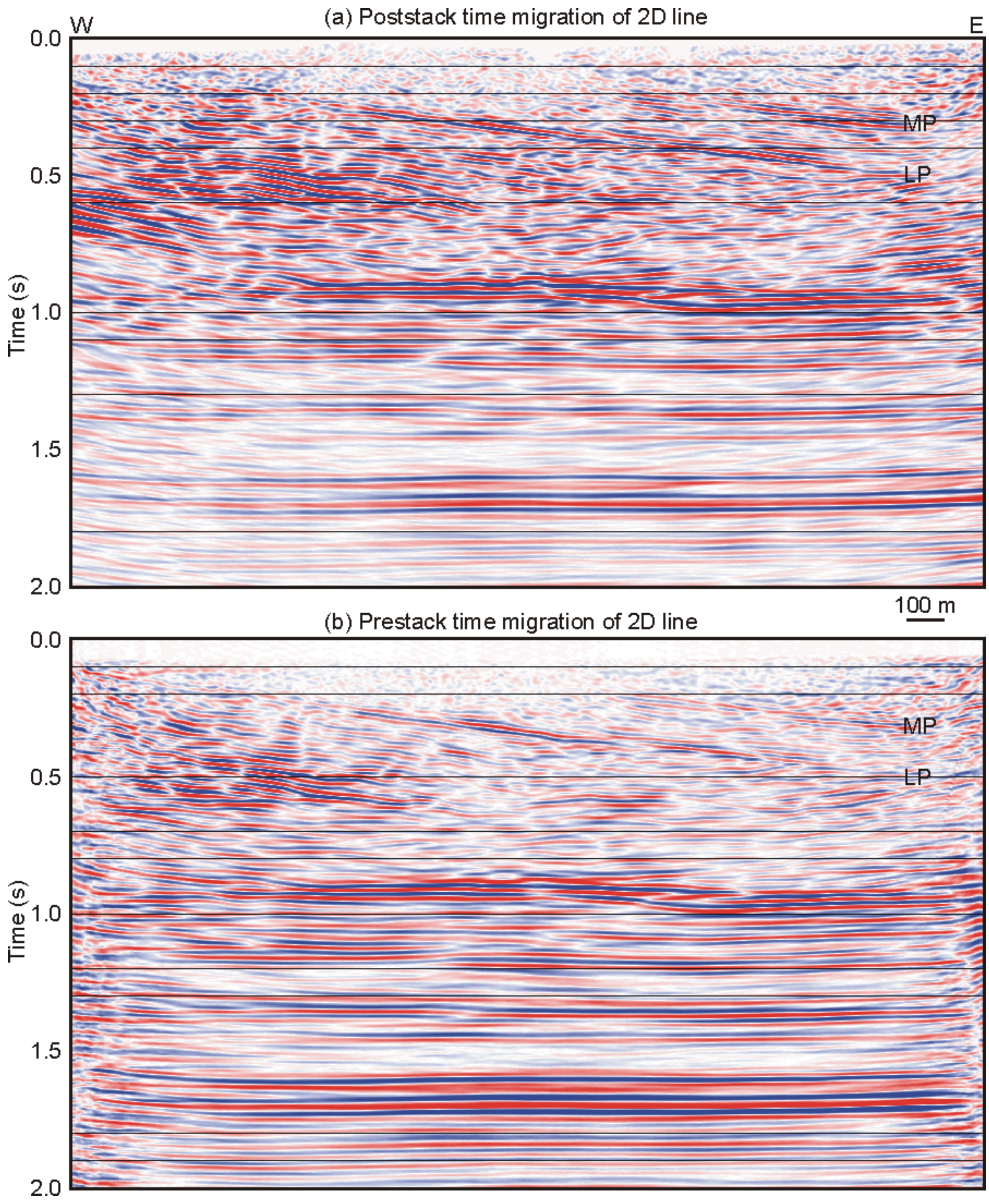

FIG. 10. (a) Poststack and (b) prestack migrations of the 2D line. The imaging of the dipping strata in the very near surface is very good in the prestack data. . MP and LP denote the Middle Paskapoo and Lower Paskapoo sands, respectively.

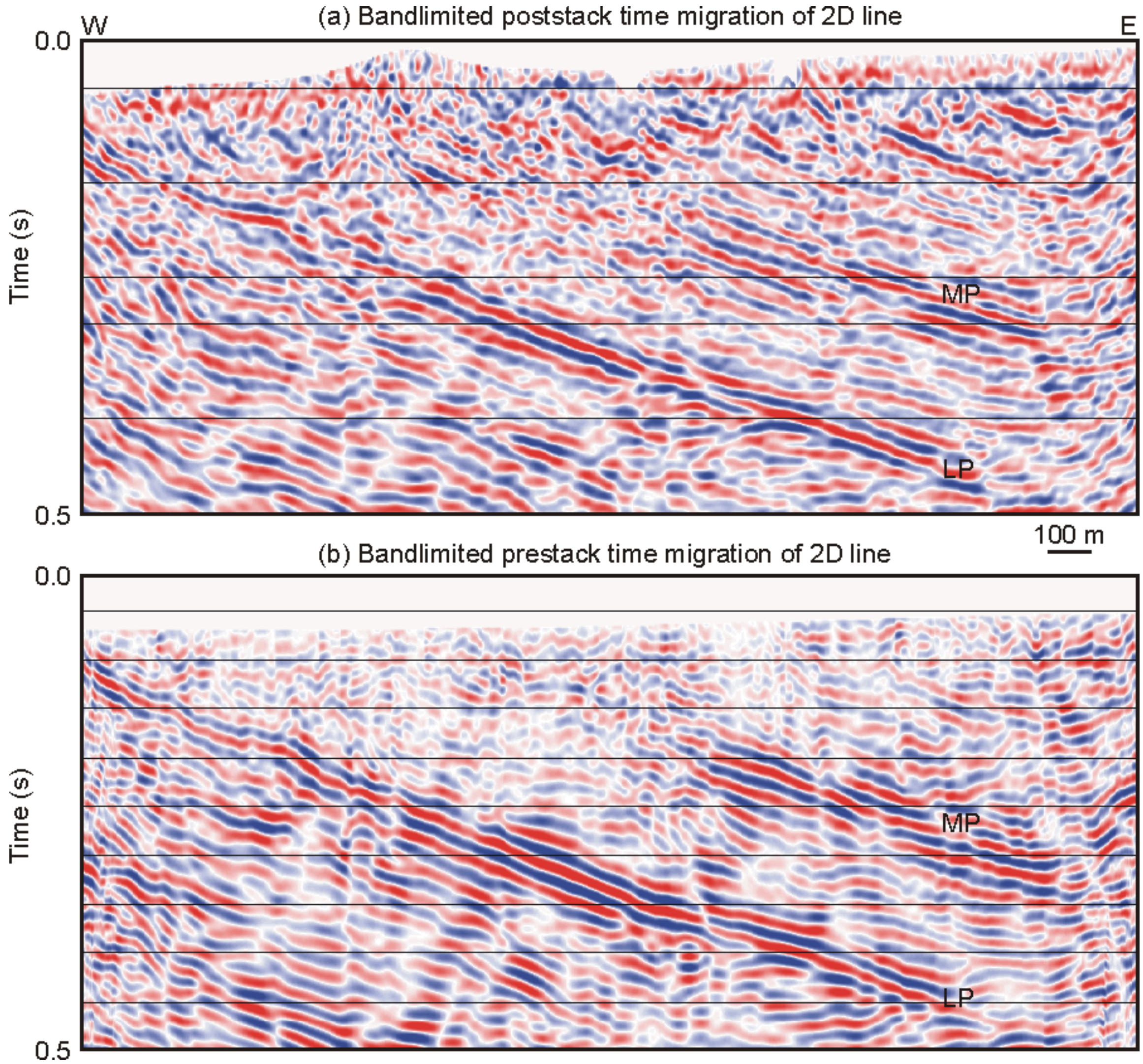

FIG. 11. Bandlimited (25-30-89-90 Hz) and zoomed versions of the migrations in Figure 10. An AGC of 300 ms has been applied. MP and LP denote the Middle Paskapoo and Lower Paskapoo sands, respectively.

SUMMARY

The vertical components of 2D3C and 3D3C seismic field school data were processed through a standard data processing stream with the purpose of attenuating noise and enhancing signal, especially in the shallow section. The best imaging is seen on the prestack migrated version of the 2D line, where the shallow dipping strata of the Paskapoo Formation and Edmonton Group are well imaged and in the western part of the line are seen almost up to the surface. This imaging of the near surface is enhanced by bandpass filtering to remove the lowest frequencies.

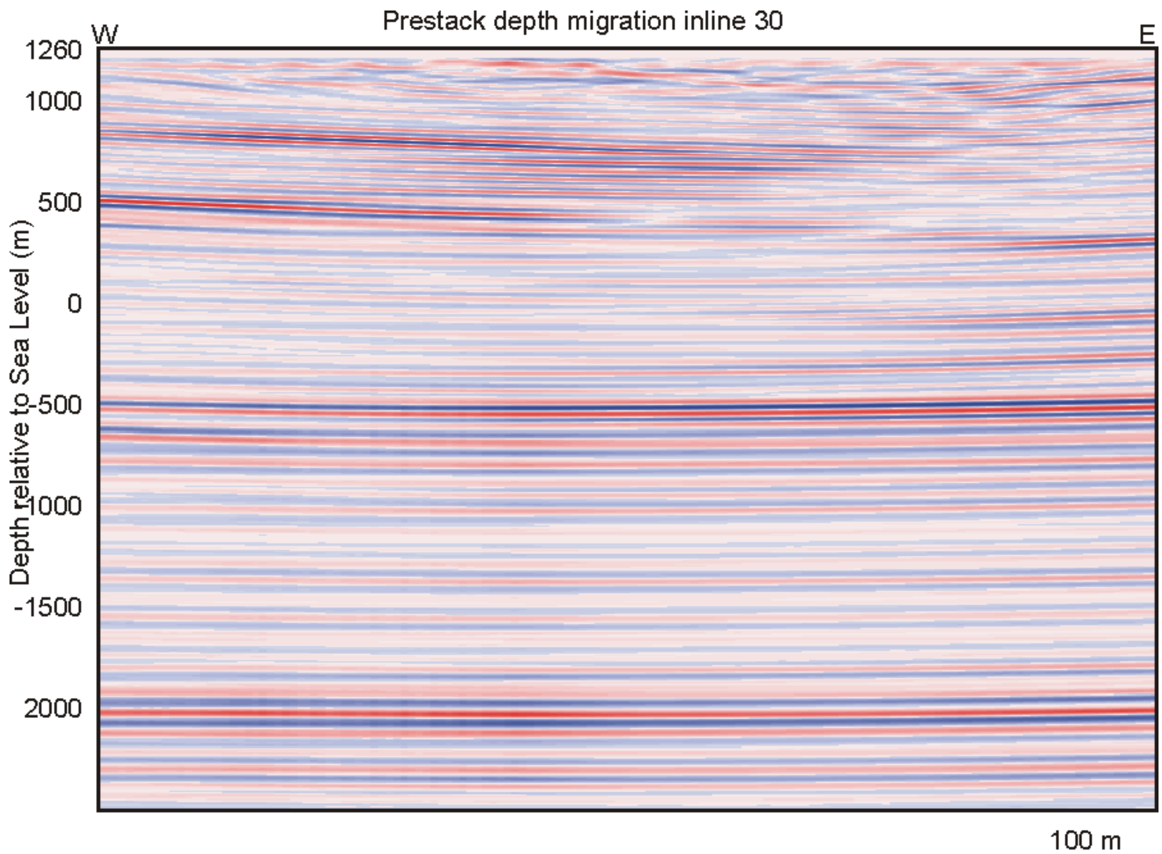

FIG. 12. Prestack depth migrated inline 30.

ACKNOWLEDGEMENTS

We would like to acknowledge the undergraduate students, graduate students, CREWES staff and faculty who acquired these seismic data. The CREWES sponsors are thanked for their support. Software suppliers (Landmark (ProMAX), Paradigm (GeoDepth), Seismic Micro-Technology, Inc (Kingdom Suite) and GlobalMapper are also thanked.

REFERENCES

Geological Survey of Canada, 1941, Geology and structure cross-sections, Fish Creek, Alberta, Map 667A, scale 1:63,360.

Hall, K. W., P. Gagliardi and D. C. Lawton, 2010, GPS accuracy part 2: RTK float versus RTK fixed: CREWES Annual Research Report, Vol. 22.

Isaac J. H. and D. C. Lawton, 2010, Integrated geological and seismic site characterization at Priddis, Alberta: CREWES Annual Research Report, Vol. 22.

Margrave, G. F. and M. P. Lamoureux, 2002, Gabor deconvolution: CSEG Annual Convention Expanded Abstracts.

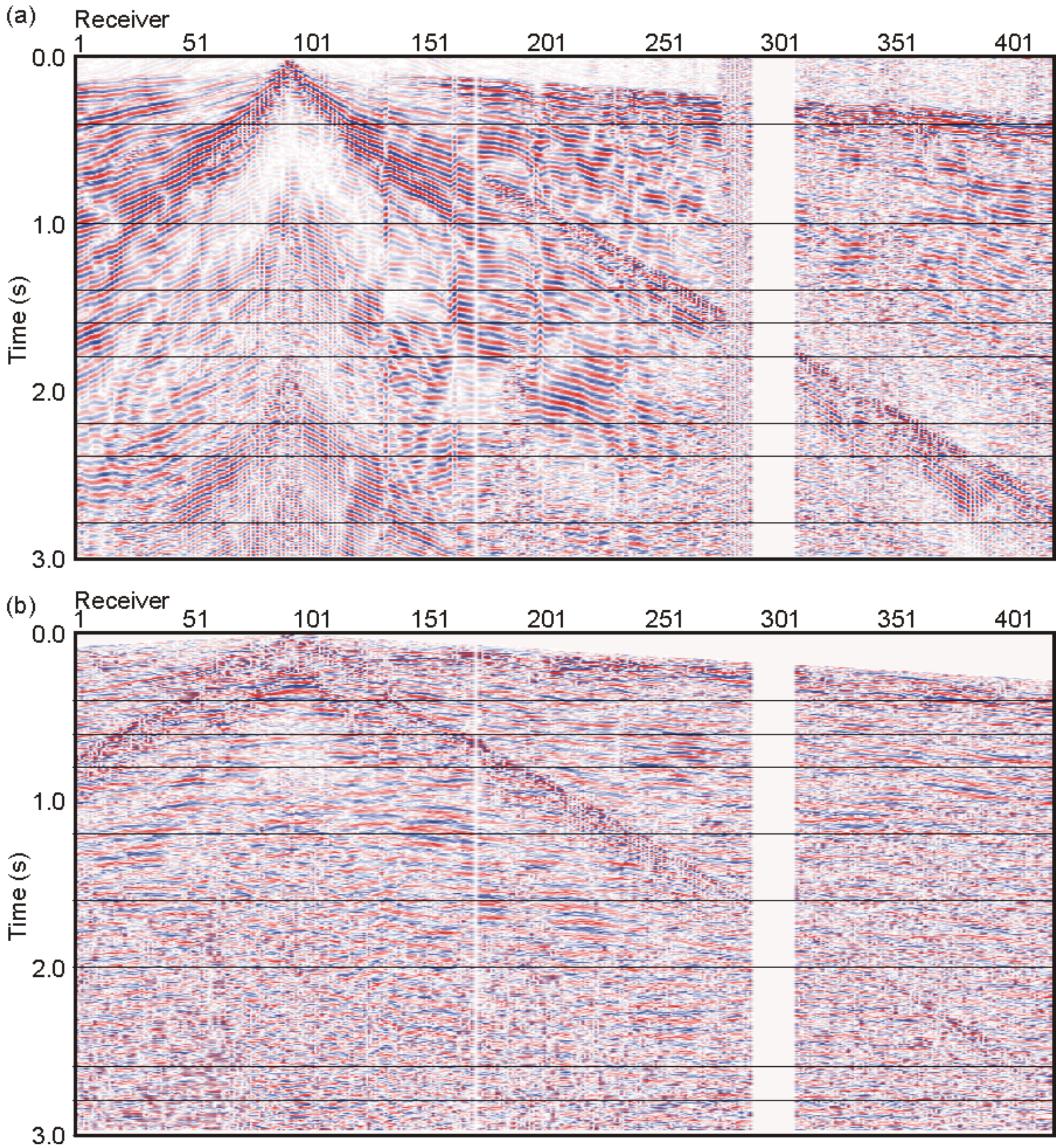

FIG. 13. Converted-wave shot gathers (a) before and (b) after some noise attenuation, elevation statics and shot refraction statics. The receiver gap occurs where the line crossed the road.